Open access • Journal Article • DOI:10.1109/TSG.2016.2633298

Active Power Quality Improvement Strategy for Grid-Connected Microgrid Based on Hierarchical Control — Source link

Wei Feng, Kai Sun, Yajuan Guan, Josep M. Guerrero ...+1 more authors

Institutions: Tsinghua University, Aalborg University

Published on: 01 Jul 2018 - IEEE Transactions on Smart Grid (IEEE)

Topics: Voltage regulator, Voltage controller, Voltage droop, Microgrid and AC power

Active Power Quality Improvement Strategy for Grid-connected Microgrid Based on Hierarchical Control

Wei, Feng ; Sun, Kai; Guan, Yajuan; Guerrero, Josep M.; Xiao, Xi

Published in:
I E E E Transactions on Smart Grid

DOI (link to publication from Publisher):
10.1109/TSG.2016.2633298

Publication date:
2018

Document Version
Early version, also known as pre-print

Active Power Quality Improvement Strategy for Grid-connected Microgrid Based on Hierarchical Control

Wei Feng, *Student Member, IEEE*, Kai Sun, *Senior Member, IEEE*, Yajuan Guan, *Student Member, IEEE*, Josep M. Guerrero, *Fellow, IEEE*, Xi Xiao, *Member, IEEE*

Abstract—When connected to a distorted grid utility, droop-controlled grid-connected microgrids (DCGC-MG) exhibit low equivalent impedance. The harmonic and unbalanced voltage at the point of common coupling (PCC) deteriorates the power quality of the grid-connected current (GCC) of DCGC-MG. This work proposes an active, unbalanced, and harmonic GCC suppression strategy based on hierarchical theory. The voltage error between the bus of the DCGC-MG and the grid's PCC was transformed to the *dq* frame. On the basis of the grid, an additional compensator, which consists of multiple resonant voltage regulators, was then added to the original secondary control to generate the negative fundamental and unbalanced harmonic voltage reference. Proportional integral and multiple resonant controllers were adopted as voltage controller at the original primary level to improve the voltage tracking performance of the inverter. Consequently, the voltage difference between the PCC and the system bus decreased. In addition, we established a system model for parameter margin and stability analyses. Finally, the simulation and experiment results from a scaled-down laboratory prototype were presented to verify the validity of the proposed control strategy.

***Index Terms*—grid-connected current; power quality; droop; distorted; unbalance; hierarchical control.**

I. Introduction

Renewable energy has drawn considerable attention in recent years because of growing concerns regarding traditional fossil energy shortages and other environmental problems. Therefore, power systems have undergone major changes not only for ensuring sustainable development but also for solving power supply problems in remote areas [1]–[2]. One such innovation is the microgrid (MG), which can integrate different kinds of energy sources and power electronics interfaced with units of distributed generations (DGs).

Over time, MGs became expected to perform even more functions and complex. Thus, an advanced MG hierarchical theory was proposed to define the system on three levels, thereby facilitating controller design depending on the different functions [3]–[4]. Although the MG's traditional hierarchical structure has been well developed over the past years, several issues have been raised as regards its practical operation, and a number of improvements have been made for the system's ancillary services [5]–[8].

The virtual impedance control loop was developed to optimize inductance-to-resistance (X/R) ratio of the inverter's equivalent output impedance. This control loop is usually added to the MG's primary control to guarantee the good performance of a regular droop controller. However, reactive load sharing precision is closely associated with voltage, rather than frequency, and the voltage along distributed lines in the MG is not constant. Therefore, a secondary controller that includes a reactive power sharing loop was proposed in [5], thus allowing the central controller to be used for improving robustness instead for distributed control strategies. Nonetheless, communication conflicts and delays would occur more frequently as the number of DGs in the MG increases, and system stability will be impeded by the communication network's bandwidth in a hierarchical-controlled MG. The margin of communication delay was investigated in [6] with a small signal model of the system, and a gain scheduling approach was proposed in that paper to compensate for the effects of communication delay in a hierarchical-controlled MG.

As the nonlinear and unbalanced loads increasing along the low voltage distribution line, the power quality issue of islanded MG has drawn considerable attention by researchers recently. Many improving control approaches for droop controlled VCIs without communication network are proposed in [9]-[11]. A cooperative harmonic filtering strategy through G-H droop was proposed in [9]. With this strategy, harmonic current can be shared precisely and the power quality of MG bus voltage can be guarantee. Harmonic current is associated with the equivalent impedance of VCIs in MG. As harmonic current increases, the occurrence risk of high-frequency resonance in MG also increases. Therefore, a resonance suppression and harmonic current sharing strategy was investigated in [10] by extending the harmonic virtual impedance control loop. Moreover, an enhanced droop control method involving online virtual impedance adjustment was proposed in [11] for autonomous islanded MG; the virtual impedance at different components and sequences were tuned on line to realize accurate power sharing.

Researchers have reported on a communication-based hierarchical control for the unbalanced and harmonic bus voltage suppression of an islanded MG. The system's harmonic

Manuscript revised Jul. 25, 2016; accepted Nov. 6, 2016. Date of publication XX XX, XX; date of current version Nov. 23, 2016. This work was supported by the National High Technology Research and Development Program (863 Program, 2015AA050606) and the program of Beijing Natural Science Foundation under grant (KZ201511232035). Paper no. TSG-00558-2016. (Corresponding author: Kai Sun.)

Wei Feng, Kai Sun, and Xi Xiao are with the State Key Lab of Power Systems, Department of Electrical Engineering, Tsinghua University, Beijing 100084, China (e-mail: fwqqrse@mail.tsinghua.edu.cn, sun-kai@mail.tsinghua.edu.cn, xiao_xi@mail.tsinghua.edu.cn).

Yajuan Guan and Josep M. Guerrero are with Department of Energy Technology, Aalborg University, 9220 Aalborg, Denmark (e-mail: ygu@et.aau.dk, joz@et.aau.dk).

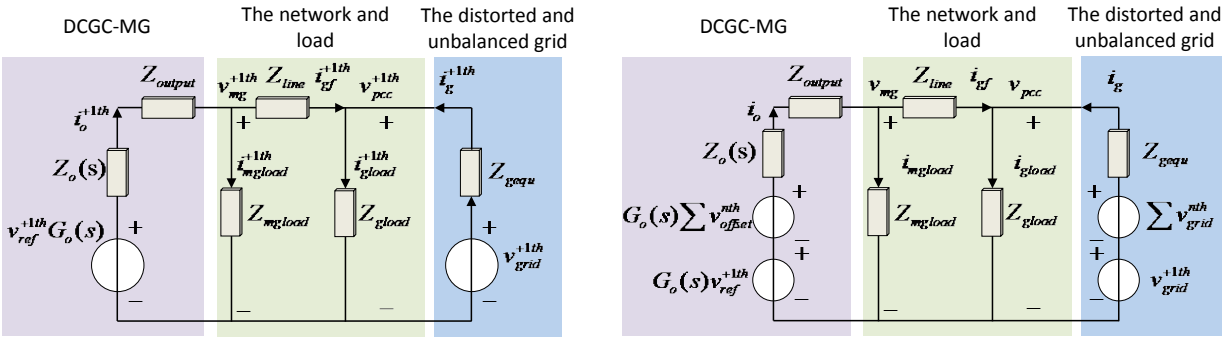

Fig. 1. The equivalent circuit of DCGC-MG. (a) System with traditional control and stiff grid, (b) System with voltage offset and distorted and unbalanced grid.

current sharing improvement was provided at the expense of increased voltage harmonic distortion. Thus, in [12], harmonic compensation was calculated using a secondary controller and then sent to inverters at the primary level. Following the same principle, the point of common coupling (PCC) unbalanced depression strategy was considered in [13]. Another voltage waveform control approach for suppressing harmonics in an islanded MG was proposed in [14], and a selective harmonic compensator was implemented in the secondary voltage control system to redistribute bus harmonic voltage distortions.

Given that the output impedance of DCGC-MG is small, the system, when connected to the grid, is equivalent to a controlled voltage source [15]–[16]. Few studies have been conducted on connecting DCGC-MG with the grid, and only a stiff grid scenario is considered in these works [17]. However, grid-connected voltage controlled inverters (GF-VCI), whose output feature is similar to that of the DCGC-MG, has been extensively investigated [18]-[20]. The control principle of GF-VCI was presented in [18], wherein multiple resonant (*R*) controllers were adopted in the voltage control loop and different voltage components of the grid were extracted by sliding discrete Fourier transform. The harmonic voltage components were then feedforward to the inner loop of the system, consequently reducing the harmonic GCC of the GF-VCI [19]. Moreover, a closed-loop triple-loop control algorithm was proposed in [20]. The error of the grid-connecting current reference generated by fundamental power reference was calculated with an outer current controller to generate the voltage reference for GF-VCI. Then, accurate grid current harmonic compensation was realized.

Analogously, the distorted grid voltage will seriously deteriorate the power quality of the GCC of the DCGC-MG. However, no study has examined the power quality of the GCC of a system connected to an unbalanced and distorted gird at PCC. Therefore, the contribution of paper is to propose a control strategy for improving the power quality of the GCC and for suppressing the harmonic GCC components when DCGC-MGs are connected to a distorted grid. In this study, a detailed steady and dynamic performance analysis is performed, as well as a parameter margin analysis based on the equivalent transfer function model. A detailed design guideline for specific and practical parameters is also provided.

This work is organized as follows. Section II presents the model of the DCGC-MG connected to the distorted grid. Section III describes the proposed control strategy based on a hierarchical structure. Section IV analyzes the steady performance and the control parameter margin. Section V discusses the experimental results. Section VI concludes the paper.

II. Modeling of the System

Fig. 1 (a) shows the simplified equivalent circuit of the DCGC-MG with a conventional control strategy when connected to the stiff grid utility. To facilitate this analysis, only one-droop controlled VCI is assumed to be present in the system, in which the droop controller generates the fundamental reference (v_{ref}^{+1th}). The VCI's voltage transfer function and the equivalent impedance is represented by $G_o(s)$ and $Z_o(s)$, respectively. A high *X/R* ratio between VCIs is guaranteed either by physical or virtual impedance (Z_{output}) when the droop law is adopted. Local loads (Z_{mgload}) are connected to the bus of the DCGC-MG. The system is connected to the stiff grid at the PCC through the line impedance (Z_{line}), where the voltage is v_{pcc}^{+1th}, and the bus voltage of the DCGC-MG is v_{mg}^{+1th}. The grid utility is modeled as an ideal voltage source with the only fundamental positive voltage (v_{grid}^{+1th}). The equivalent line impedance of the grid is Z_{gequ}. The fundamental GCC (i_{gf}^{+1th}) can be calculated as follows:

$$i_{gf}^{+1th} = \frac{v_{mg}^{+1th} - v_{pcc}^{+1th}}{Z_{line}} \tag{1}$$

However, when unexpected harmonic and unbalanced voltage disturbances occur at the grid, the grid can be denoted as the sum of v_{grid}^{+1th} and other components ($\sum v_{grid}^{nth}$), at which point the voltage and current in the model can be decomposed as corresponding positive and negative sequences based on the method of symmetrical components. The magnitude of the negative fundamental or harmonic GCCs can be calculated based on the superposition theorem as follows:

$$\left|i_{gf}^{nth}(j\omega_b^{nth})\right| = \left|\frac{v_{mg}^{nth}(j\omega_b^{nth}) - v_{pcc}^{nth}(j\omega_b^{nth})}{Z_{line}(j\omega_b^{nth})}\right|_{n=-1,\pm5,\pm7\ldots} \tag{2}$$

being:

$$v_{mg}^{nth}(j\omega_b^{nth}) = v_{ref}^{nth}G_o(j\omega_b^{nth}) - i_o^{nth}[Z_o(j\omega_b^{nth}) + Z_{output}(j\omega_b^{nth})]$$
$$v_{pcc}^{nth}(j\omega_b^{nth}) = v_{grid}^{nth}(j\omega_b^{nth}) - i_g^{nth}Z_{gequ}(j\omega_b^{nth})$$

where, i_{gf}^{nth}, i_o^{nth}, i_g^{nth} are the negative fundamental or harmonic components of the GCC, inverter output current, and main grid current, respectively; v_{mg}^{nth}, v_{grid}^{nth}, v_{pcc}^{nth}, and v_{ref}^{nth} are the negative fundamental or harmonic components of the MG bus's voltage, the grid voltage, the PCC voltage at the grid side, and the offset voltage, respectively. Here, ω_b^{nth} is the angular frequency.

The original control loops of droop-based VCIs are designed to maintain the positive fundamental component of the voltage. As such, the closed loop gain at the harmonic angular frequency of VCIs is very small, specifically $G_o(j\omega_b^{nth}) << 0dB$. Moreover, no negative fundamental or unbalanced harmonic components of grid voltage are directly sent back to the primary control. The DCGC-MG is almost a shortcut to the corresponding frequency when connected to the distorted grid. The amplitude of the negative fundamental and harmonic GCC can be approximated as follows:

$$\left|i_{gf}^{nth}(j\omega_b^{nth})\right| = \left|\frac{-v_{imped}^{nth}(j\omega_b^{nth}) - v_{pcc}^{nth}(j\omega_b^{nth})}{Z_{line}(j\omega_b^{nth})}\right|_{n=-1,\pm5,\pm7...} \quad (3)$$

As shown in (3), the distortion of the GCC of the DCGC-MG is inevitable unless an additional control is adopted. However, the proposed compensator in the secondary control is responsible for generating an additional harmonic and unbalanced voltage offset (Fig.1 (b)) to reduce the voltage difference in the corresponding components across the line impedance, as shown in (4). In other words, the distorted and unbalanced GCC can be suppressed by decreasing the numerator in (4). Therefore, the system can be improved by generating and tracking the appropriate voltage offsets.

$$\left|i_{gf}^{nth}(j\omega_b^{nth})\right| = \left|\frac{v_{offset}^{nth}G_o(j\omega_b^{nth}) - v_{imped}^{nth}(j\omega_b^{nth}) - v_{pcc}^{nth}(j\omega_b^{nth})}{Z_{line}(j\omega_b^{nth})}\right|_{n=-1,\pm5,\pm7...} \quad (4)$$

III. Proposed Power Quality Improving Strategy

A. Improved primary control level

Because the voltage compensating offsets are transmitting to the VCIs at the primary level, two improvements are made to the original control loop. The DC offset signals in the *dq* frame are adopted to decrease the bandwidth requirements of the communication network. Therefore, the DC offset signals are transformed back to the *abc* frame by the different inverters in the primary control. The other improvement is that the tracking performances of all components are improved to generate accurate voltage offset at the output of each VCIs, as shown in Fig. 2.

Located at the primary control level are the VCI's inner voltage/current control loop, the virtual impedance control loop, and the well-known droop controller. The angle (θ_{inv}^{+1th}) and amplitude (E_{inv}^{+1th}) of VCIs' fundamental voltage reference is generated by the droop controller, as shown below:

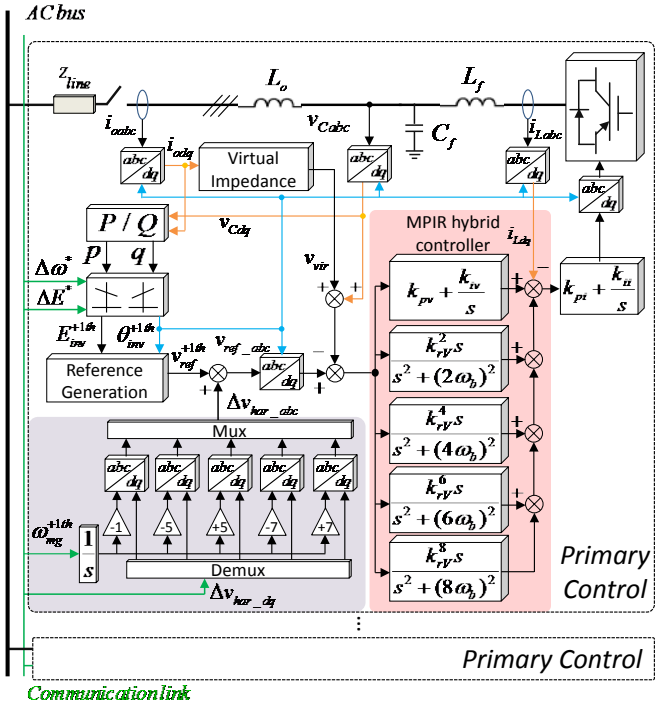

Fig. 2. The improved control strategy in the primary level

$$\begin{cases}\theta_{inv}^{+1th} = \int\left[\omega_b^* + \Delta\omega^* - m_p(P^* - G_{LPF}(s)p)\right]dt \\ E_{inv}^{+1} = E_b^* + \Delta E^* - m_q\left[Q^* - G_{LPF}(s)q\right]\end{cases} \quad (5)$$

where m_p and m_q are droop parameters for active power and reactive power, respectively; P^* and Q^* are the rated active and reactive power of the inverters, and ω_b^* and E_b^* represent the rated angular frequency and amplitude of the fundamental component. $\Delta\omega^*$ and ΔE^* are the angular frequency and the amplitude of fundamental increments transferred through the communication link. $G_{LPF}(s)$ is a regular low pass filter (LPF), which smoothes the calculated instantaneous power (p and q) and provides more damping to the system.

The restoring and synchronization controllers at the secondary control level and the power flow controller at the tertiary control level will be switched in the islanded mode or the grid-connected mode of the system, respectively. Therefore, $\Delta\omega^*$ and ΔE^* are calculated differently depending on the system's operation mode, as follows:

$$\Delta\omega^* = \begin{cases}\Delta\omega_{syn}^{+1th} + \Delta\omega_P^{+1th} & (Grid-connecting) \\ \Delta\omega_{rest}^{+1th} & (Islanded)\end{cases} \quad (6a)$$

$$\Delta E^* = \begin{cases}\Delta E_{syn}^{+1th} + \Delta E_Q^{+1th} & (Grid-connecting) \\ \Delta E_{rest}^{+1th} & (Islanded)\end{cases} \quad (6b)$$

where $\Delta\omega_{syn}^{+1th}$ and ΔE_{syn}^{+1th} are the outputs of the synchronization controller, $\Delta\omega_{rest}^{+1th}$ and ΔE_{rest}^{+1th} are the outputs of the restoring controller in the secondary control.

The DC offset signals in the *dq* frame based on ω_b^{nth} must be transformed back to the *abc* frame to combine the final three-phase voltage reference (v_{ref_abc}) of the VSIs as follows:

$$\begin{cases} v_{ref\_a} = E_{inv}^{+1th}\sin(\theta_{inv}^{+1th}) + \Delta v_{har\_a} \\ v_{ref\_b} = E_{inv}^{+1th}\sin(\theta_{inv}^{+1th} - 2\pi/3) + \Delta v_{har\_b} \\ v_{ref\_c} = E_{inv}^{+1th}\sin(\theta_{inv}^{+1th} + 2\pi/3) + \Delta v_{har\_c} \end{cases} \quad (7)$$

where Δv_{har_abc} is the voltage offset in the *abc* frame that is generated by the proposed compensator.

Then, v_{ref_abc} is transformed to the *dq* frame with θ_{inv}^{+1th} for the inner voltage/current controllers of the VCI. Given that DC components and $2n^{th}$ harmonic components are present in the voltage offset in the *dq* frame, a hybrid controller consisting of a regular proportional integral (*PI*) controller and multiple *R* controllers (PIMR) is adopted as the voltage control loop, shown in (8). The use of the PIMR voltage controller is advantageous as it will improve the power quality when the DCGC-MG is operated under islanded mode with nonlinear loads [21]–[22].

$$G_v = k_{pv} + \frac{k_{iv}}{s} + \sum_{n=2,4,6..} \frac{k_{rv}^{nth}}{s^2 + (n\omega_b)^2} \quad (8)$$

where k_{pv} and k_{iv} are the control parameters of the regular *PI* controller, and k_{rv}^{n} is the integral parameter for *R* controller.

B. Improved secondary control level

The system's improved secondary control level is depicted in Fig. 3. The conventional frequency/amplitude restoring controller in the islanded mode and the synchronization controller in the grid-connected mode have been discussed thoroughly in previous works [5], [8].

However, even when the PIMR voltage controller is adopted at the primary level, the system's GCC will still be distorted by the inevitable harmonic and unbalanced voltage differences between the PCC and the system bus. Therefore, to overcome this problem, a harmonic and unbalanced compensator is introduced at the secondary level to eliminate the corresponding voltage differences and improve the power quality of the GCC, as shown in Fig. 4. When Park transformation is applied, the three-phase error voltage with an angular frequency of $n\omega_b$ in the *abc* frame can be transformed to sine and cosine signals in the *dq* frame. Therefore, multiple parallel *R* controllers are adopted, as shown in (9).

$$G_{r\_sec}(s) = \sum_{n=2k} G_{r\_sec}^{nth}(s) = \sum_{n=2k} \frac{k_{r\_Sec}^{nth} s}{s^2 + (n\omega_b)^2} \quad (9)$$

where $k_{r\_Sec}^{nth}$ is the control parameter of *R* controllers for different harmonic components.

The *R* controllers with resonant angular frequencies of $2\omega_b$, $4\omega_b$ and $8\omega_b$ are used to compensate for the negative 1st, positive 5th, negative 7th components in the *abc* frame, respectively, while the *R* controller with resonant angular frequency of $6\omega_b$ is used to compensate for the negative 5th and positive 7th components. The specific harmonic component selection and calculation are realized through the infinite gain of the corresponding *R* controller at the resonant angular frequency, which is attenuated sharply at the other angular

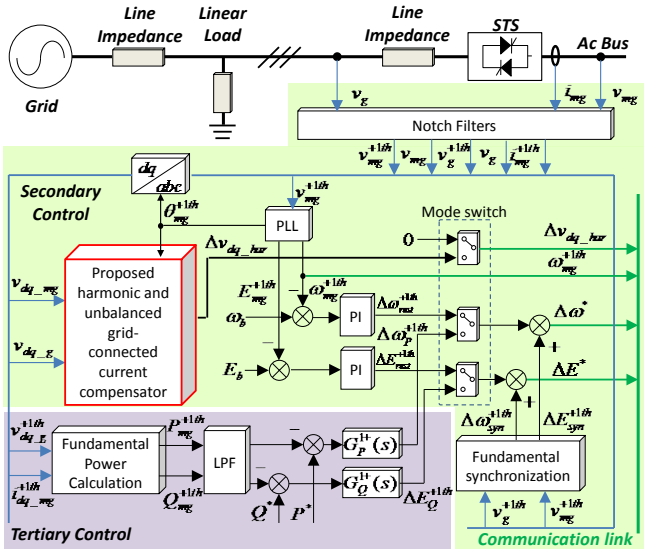

Fig. 3. The tertiary and improved secondary control for DCGC-MG with the proposed compensator

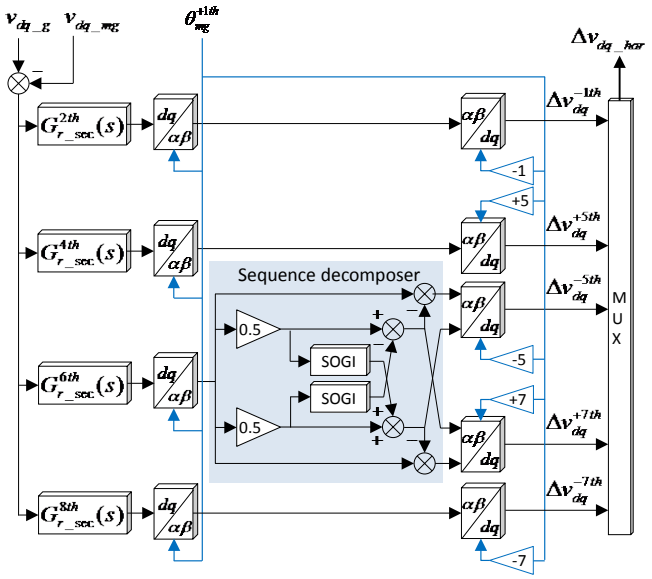

Fig. 4 The proposed compensator in the secondary level

frequency. Therefore, no additional harmonic component estimators are needed, and the proposed control strategy can be implemented with minor calculation requirements.

To transform the offset signal to the DC signal, the output of *R* controllers are first transformed to the $\alpha\beta$ frame with an angular frequency of ω_b and then transformed to the DC signal by using Park transformation with the corresponding angular frequency and sequence, as shown in Fig. 4. Therefore, a regular sequence decomposer based on the 1/4 delay method is adopted for extracting the positive and negative 6th signals from the output of $G_{r\_sec}^{6th}(s)$, in which a second-order generalized integrator (SOGI) is used for the phase delay, as shown below:

$$G_{SOGI}(s) = \frac{k(6\omega_b)^2}{s^2 + 6ks\omega_b + (6\omega_b)^2} \quad (10)$$

where k is the coefficient affecting the SOGI's bandwidth.

The negative fundamental and unbalanced harmonic voltage offsets are then sent back to the primary control level. The

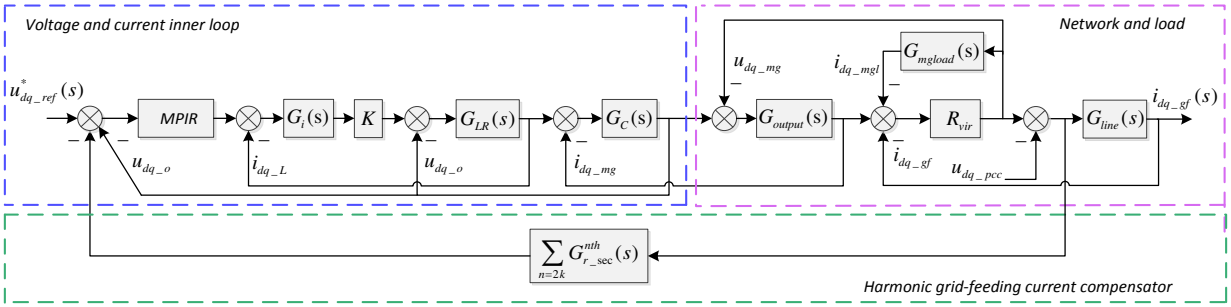

Fig. 5. The equivalent control model in the *dq* frame

proposed compensator is switched on when the DCGC-MG synchronizes with the distorted grid, and is switched off when the MG is converted to islanded mode.

IV. Performance and Parameter Margin Analysis

To analyze the performance and parameter margin of the proposed compensator, the proposed compensation loop ismade equivalent to another outer voltage loop of the VCI. Considering that the control parameters of the PIMR controller and the proposed compensator will affect system stability as well as grid-connected harmonic and unbalanced current suppression performance in coupling, an equivalent control model is established in the *dq* frame, as shown in Fig.5.

The fundamental positive reference of the VCI is generated by the droop controller, and this analysis focuses on the system's negative and harmonic components. Therefore, the droop control loop is omitted, and all the coupling items resulting from the Park transformation are ignored to simplify the analysis. The control model is divided into three parts. The first part consists of the inner voltage/current controller and the inverter's L_fC_f filter ($G_{LR}(s)$ and $G_C(s)$). The three-phase inverter is modeled again as (K). The second part consists of the local loads ($G_{mgload}(s)$), the line impedance between the VCI and the system bus ($G_{output}(s)$), and the line impedance between the system bus and PCC ($G_{line}(s)$). A virtual infinite resistor (R_{vir}) is added to ensure that a numerical solution can be derived. The third part is the proposed offset compensator. We ignore the harmonic and sequence decomposer at the secondary control level, the re-composer in the primary control, and the communication link delay. We assume that the output of the compensator can be accurately sent to the primary level. Therefore, the controller parameters affect the steady-state performance only. The model's input is the voltage reference in the *dq* frame ($u^*_{dq\_ref}(s)$), the output is the GCC of the DCGC-MG ($i_{dq\_gf}(s)$), and the disturbance is the distorted grid voltage ($u_{dq\_pcc}(s)$), as shown below:

$$i_{dq\_gf}(s) = G(s)u^*_{dq\_ref}(s) + \Phi(s)u_{dq\_pcc}(s) \tag{11}$$

where $G(s)$ is the voltage transfer function of inverter, which mainly represents the influence of the fundamental positive reference generated by the local droop controller to the DCGC-MG's GCC, and $\Phi(s)$ is the disturbance transfer function, which mainly denotes the influence of the harmonic voltage of the grid on the corresponding components of GCC.

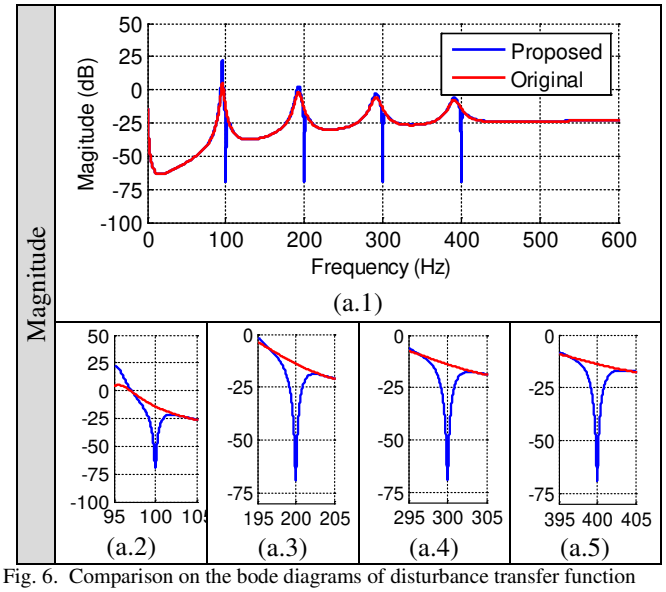

Fig. 6. Comparison on the bode diagrams of disturbance transfer function

The details of $\Phi(s)$ is provided in the Appendix.

Fig. 6 shows the comparisons of the disturbance transfer functions. As shown, with the proposed compensator, the DCGC-MG's amplitude–frequency characteristic is attenuated at the angular frequency of $2n\omega_b$ in the *dq* frame when compared to the conventional system with only the PIMR voltage controller. Therefore, the grid-connected harmonic and unbalanced currents in the *abc* frame can be impeded accordingly. Considering that the suppression performance of the $2n^{th}$ harmonic GCC in the *dq* frame is affected by both the parameters of the PIMR controller and the proposed compensator, we can estimate the steady performance by the magnitude of $\Phi(s)$ in frequency domain, as follows:

$$\begin{aligned} \left|i_{dq\_gf}(s)\right| &= \left|\Phi(s)u_{dq\_pcc}(s)\right| \\ &= f(k^{nth}_{r\_Sec}, k^{nth}_{rV}) \end{aligned} \tag{12}$$

being:

$$s = jn\omega_b,\ u_{dq\_pcc}(s) = \sum_{n=2,4,6,8} \frac{v^n_{dq} n\omega_b}{s^2 + (n\omega_b)^2}$$

where $k^{nth}_{r\_Sec}$ and k^{nth}_{rV} are the resonant control parameter in the proposed compensator and in the PIMR voltage controller, respectively; and v^n_{dq} is the disturbance voltage's amplitude in the grid utility.

Fig. 7 shows the simulation results of (12), which are

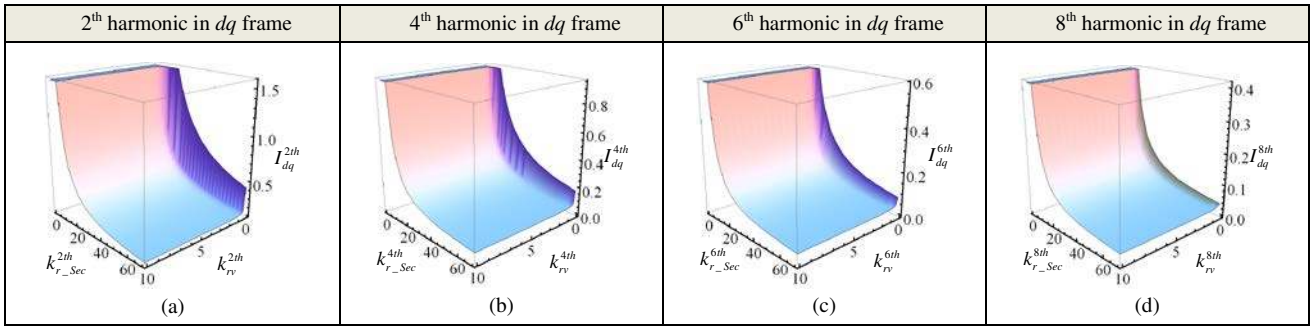

Fig. 7. The comparison on steady-state suppression performance.

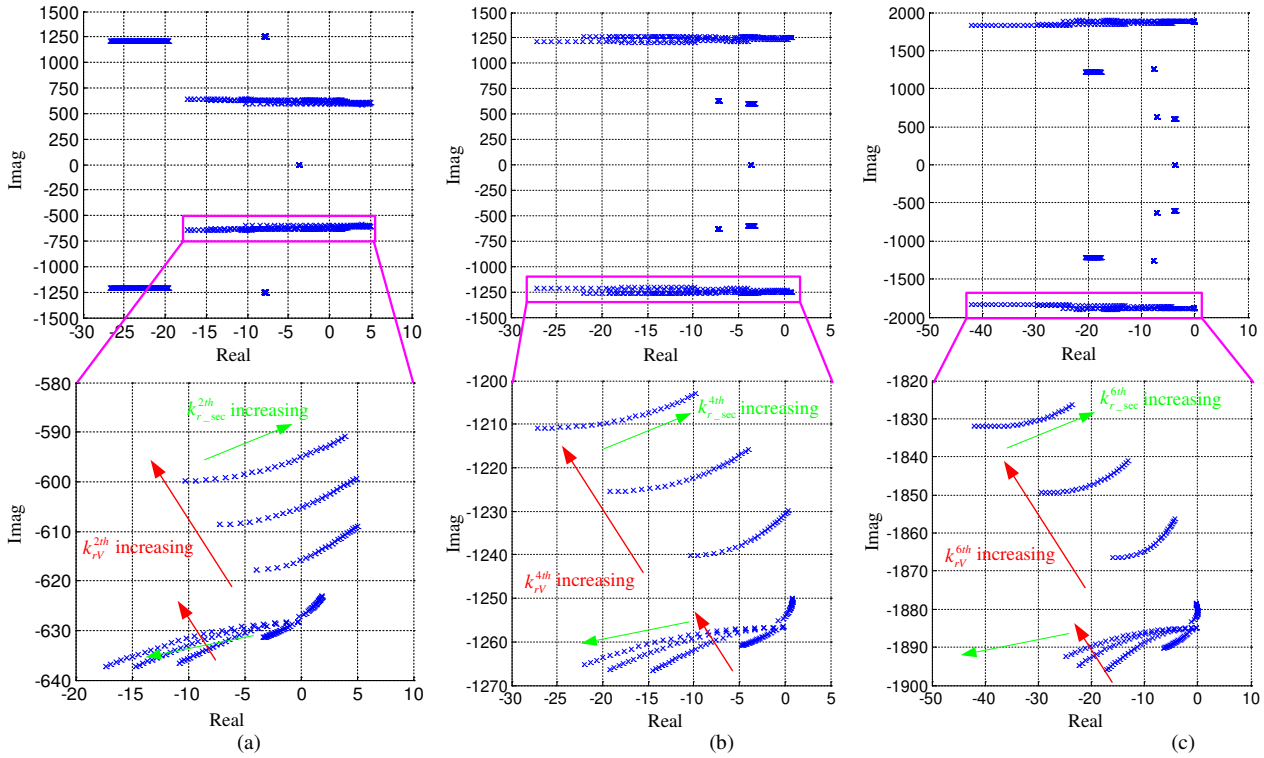

Fig. 8. Trace of modes as a function of resonant term for the PIMR voltage controller and the proposed compensator: (a) The latent root of λ_{20} and λ_{22} when $1<k_{r\_Sec}^{2th}<100$ and $1<k_{rV}^{2th}<40$, (b) The latent root of λ_{15} and λ_{17} when $1<k_{r\_Sec}^{4th}<100$ and $1<k_{rV}^{4th}<40$, (c) The latent root of λ_{11} and λ_{13} when $1<k_{r\_Sec}^{6th}<100$ and $1<k_{rV}^{6th}<40$.

conducted under the same harmonic voltage amplitude with different angular frequencies of $2n\omega_b$ in the *dq* frame. Based on the results, the following conclusions can be drawn:

- The $2n^{th}$ of GCC in the *dq* frame decreases as *n* increases even without the suppression control, mainly because the equivalent harmonic impedance is increasing while the angular frequency is increasing.
- The $2n^{th}$ of GCC in the *dq* frame cannot be suppressed by the PIMR voltage controller at primary control level alone, even with greater control parameters, because no corresponding voltage reference which presents the difference between the PCC and the bus of DCGC-MG is sent back to the primary controller.
- With the proper voltage tracking ability available in the primary control, the 2nth harmonic GCC are suppressed effectively when the compensator‘s control parameters are increasing. Otherwise, the suppression performance will be compromised. The reason is that the harmonic voltage reference generated by the compensator should be properly tracked by VCIs to decrease the correspondent voltage error between the bus of DCGC-MG and grid’s PCC.

Aside from the steady-state performance of the compensator, system stability is another important issue. The root locus based on different $k_{r\_Sec}^{nth}$ and k_{rV}^{nth} at $2n^{th}$ harmonic components in the *dq* frame are plotted to analyze the control parameter margins for DCGC-MG. As shown in Fig.8 (a), two pairs of conjugate poles are mainly involved when the resonant terms of the PIMR voltage controller and the proposed compensator are changing. λ_{20} and λ_{22} are moving away from each other as $k_{r\_Sec}^{2th}$ increases, causing the pole to move across the imaginary

TABLE I
THE PARAMETERS OF POWER STAGE AND CONTROL SYSTEM

	Item	Description		Item	Description		Item	Description	
Electrical Circuit	V_{dc}	DC Voltage	650V	f	MG Frequency	50 Hz	C_f	Filter Capacitance	9.9 μF
	V_{MG}	MG Voltage	311 V	L_f	Filter Inductance	1.8 mH	L_{line}	Line Inductance	1.8 mH
Loads	P_{reg}	P of regular load	2.2 kW	P_{sen}	P of sensitive load	0.3 kW			
	Q_{reg}	Q of regular load	0 Var	Q_{sen}	Q of sensitive load	0 Var			
Primary	k_{pi}	Current P term	0.8	K_{iv}	Voltage I term	50	k_{rv}^{4th}	4th PR integral term	40
	K_{pv}	Voltage P term	0.7	k_{rv}^{2th}	2th PR integral term	35	k_{rv}^{6th}	6th PR integral term	40
	k_{rv}^{8th}	8th PR integral term	40	m_q	Droop Q term	0.02			
	m_p	Droop P term	1e-4	ω_c	LPF time coefficient	50			
Secondary	k_{rSec}^{2th}	2th PR integral term	35	k_{rSec}^{6th}	6th PR integral term	45			
	k_{rSec}^{4th}	4th PR integral term	40	k_{rSec}^{8th}	8th PR integral term	50			
Tertiary	k_{pP}	P for Q_{mg}	2e-4	k_{dP}	D for P_{mg}	2e-6	k_{iQ}	I for Q_{mg}	1e-2
	k_{iP}	I term for P_{mg}	2e-3	k_{pQ}	P for Q_{mg}	1e-3	k_{dQ}	D for Q_{mg}	2e-6

axis and making the system unstable. However, the poles of λ_{20} and λ_{22} move close to the real axis as k_{rV}^{2th} increases, also causing the poles to move across the imaginary axis when $k_{r\_Sec}^{2th}$ becomes sufficiently large. The situation for the 4th and 6th harmonic controllers in the *dq* frame are similar, except that the resonant parameter margins for both resonant controllers in the PIMR and the proposed compensator are enlarged as the order increases.

V. EXPERIMENTAL VERIFICATION

A scaled-down experimental setup consisting of two Danfoss 2.2 kW inverters, a real-time dSPACE1006 platform, L_fC_f filters, line impedance, and two resistive loads is built, as shown in Fig. 9. One inverter is used for emulating the distorted and unbalanced grid, whereas the other two are controlled as the DCGC-MG for verifying the validity of proposed control strategy. The electrical setup and the control system parameters are listed in Table I.

Considering that the purpose is to test DCGC-MG (with or without the proposed control strategy) when it is connected to the distorted grid, the magnitude and angular frequency of harmonic components of the distorted grid voltage are set based on a general assumption that the low frequency harmonic components resulting from non-linear and single phase loads cover the main part of the distorted PCC voltage, and the magnitude of harmonic voltage components are attenuated as the order increases, as shown in Fig. 10 (a). The harmonic analysis reveals that there are negative 1st, positive and negative 5th, positive and negative 7th components, and so on in the grid voltage. The details are shown in Fig.10 (b).

The GCC of the DCGC-MG and the output current of the two VCIs when the system is connected to the distorted grid without the proposed compensator are shown in Figs. 11 (a.1), (a.2), and (a.3), and the results of the harmonic analysis are shown in Figs. 11 (b.1), (b.2), and (b.3). The GCC is highly distorted because of the existing harmonic voltage difference between the PCC and the DCGC-MG's bus. Moreover, the output harmonic current of the VCIs affects its output voltage and the system's bus voltage, further deteriorating the power quality of the output current of the VCIs. However, when the fundamental and harmonic voltage components between the PCC and the DCGC-MG's bus is decreased, and when

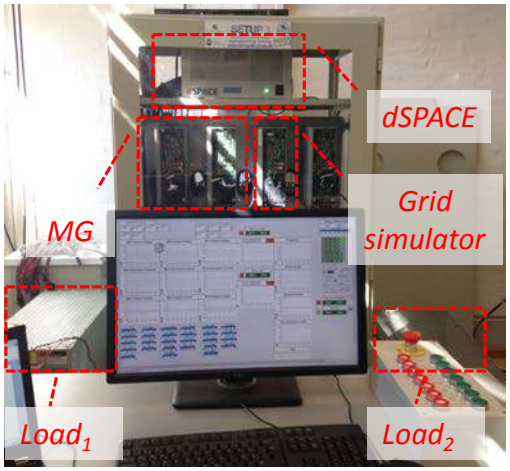

Fig. 9. The scaled-down experimental setup.

the proposed compensator is adopted, the difference of fundamental and harmonic voltage components between PCC and DCGC-MG's bus is decreased and the power quality of the GCC is improved, as shown in the Fig.11 (c.1). The negative fundamental, positive, and negative 5th and 7th components of the GCC are decreased to approximately 0.05, 0.025, and 0.02 A. The low output harmonic current will also improve the operation of the droop controller. Therefore, the output current of the VCIs is improved. The harmonic analyses are shown in detail in Figs. 11 (d.1), (d.2) and (d.3).

However, as the grid is distorted dynamically in reality, another scenario is used to test the dynamic response of the proposed control strategy, as shown in 12. The DCGC-MG is connected to the ideal grid at 0 s. The peak value of the GCC is 3.65 A. As shown in subfigure #1 in Fig. 12, the power quality of the GCC is high at 0 s. When the distorted voltage disturbance is added to the grid at 0.8 s, the GCC becomes distorted, as shown in subfigure #2 in Fig. 12. However, the proposed compensator only takes 2.7 s to generate the appropriate voltage offset to improve the power quality of the GCC, as shown in subfigure #3 in Fig. 12. Step down testing is also conducted on the distorted grid voltage disturbance at 7.5 s The same phenomenon is observed in the system. Although the GCC is distorted during the dynamic response, the power quality of the GCC will be guaranteed when the system with proposed control strategy returns to a stable point.

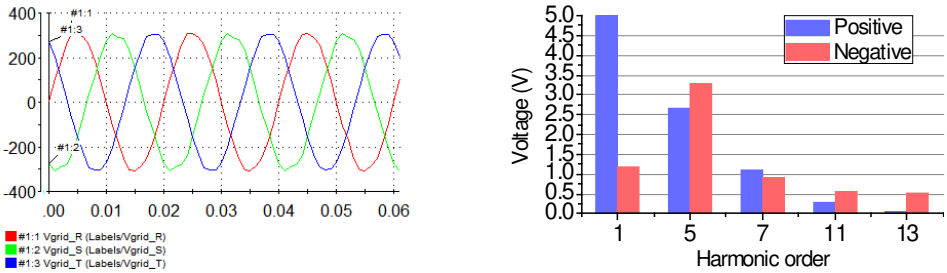

(a) (b)

Fig. 10. The 3 phase distorted grid voltage in experiments. (a) The waveform of voltage, (b) The voltage harmonic analysis.

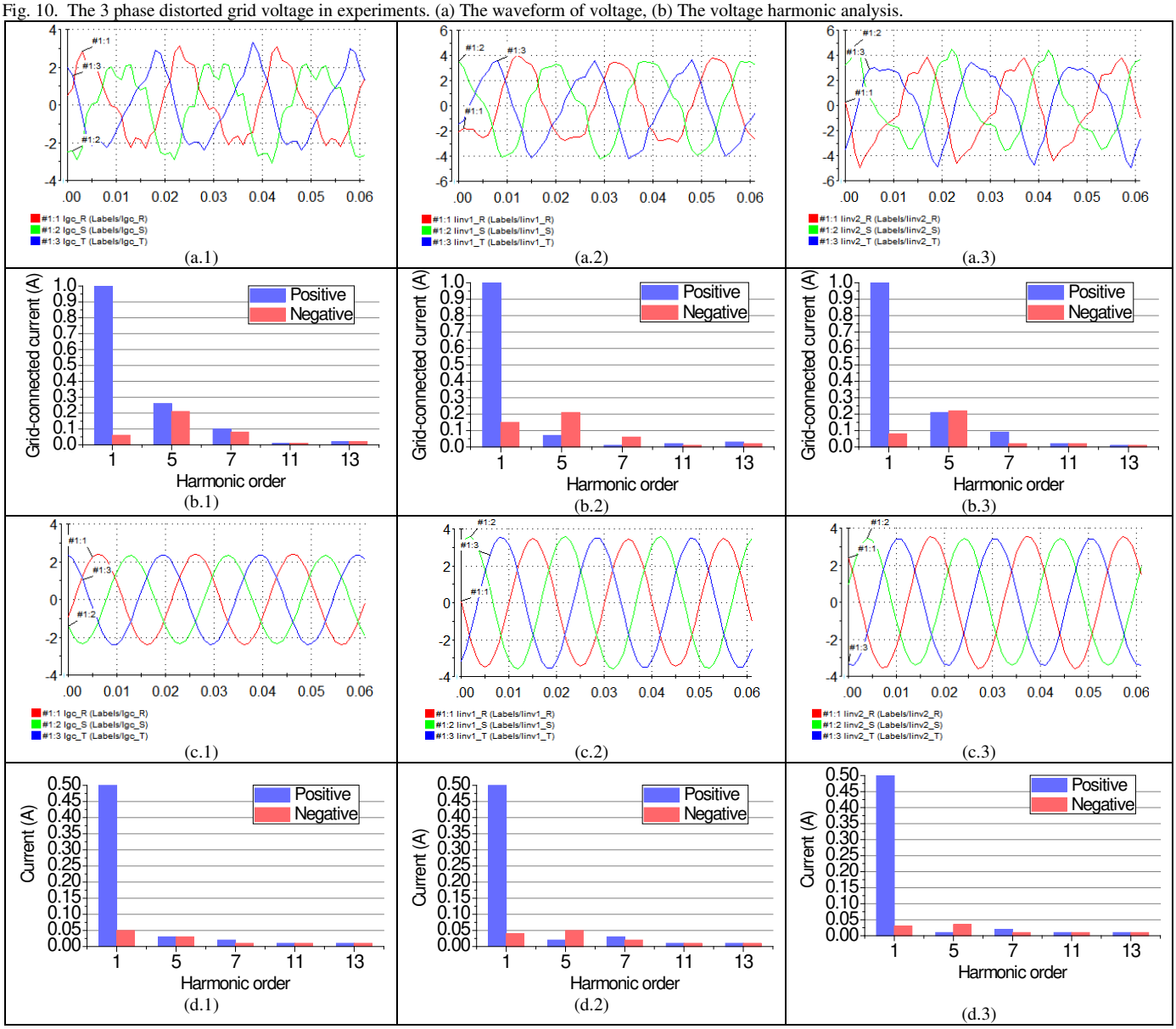

Fig. 11. The dynamic response of the proposed control strategy.

VI. . CONCLUSIONS

This work developed an active harmonic and unbalanced GCC compensation strategy based on hierarchical theory for the DCGC-MG. The voltage error between the bus of the system and the PCC was transformed to the *dq* frame, and an additional compensator consisting of multiple *R* voltage controllers were added to the original secondary control to generate the negative fundamental and harmonic voltage offset of the VCIs in the primary control. PIMR controllers were adopted as voltage controllers at the original primary level to improve the VCI's voltage tracking performance. Consequently, the corresponding voltage component differences between the PCC and the bus of the DCGC-MG decreased significantly, thus improving the power quality of the GCC. Experimental results were included to validate the excellent behavior of the proposed compensation strategy.

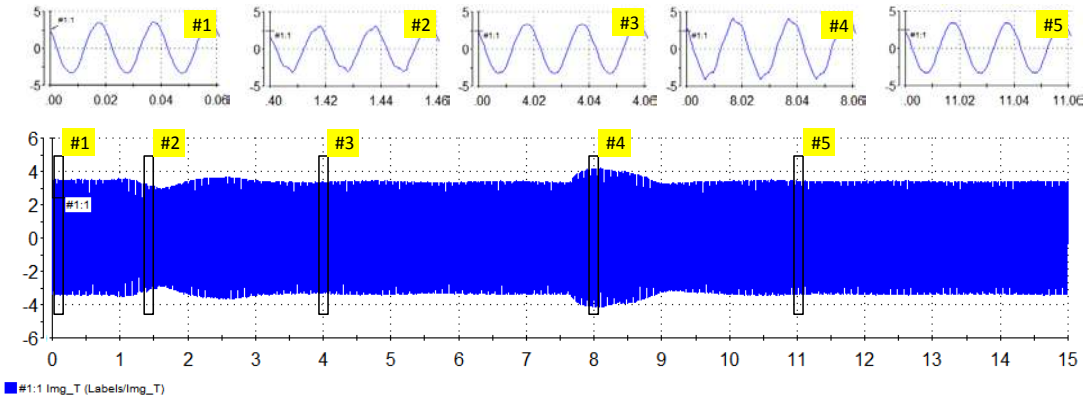

Fig. 12. The dynamic response of the proposed control strategy.

APPENDIX

The detailed of disturbance transfer in Section IV is shown as follows:

$$\Phi(s)=\frac{\alpha}{\beta} \quad \text{(A.1)}$$

Where:

$$\alpha=-G_{line}-G_cG_{line}G_{LR}-G_cG_{line}G_{output}-G_iG_{line}G_{LR}K-G_cG_iG_{line}G_{LR}G_{output}K-G_cG_iG_{line}G_{LR}G_vK-G_{mgload}R_{vir}-G_cG_{LR}G_{mgload}R_{vir}$$
$$-G_{line}G_{output}R_{vir}-G_cG_{line}G_{LR}G_{output}R_{vir}-G_cG_{mgload}G_{output}R_{vir}-G_iG_{LR}G_{mgload}KR_{vir}-G_iG_{line}G_{LR}G_{output}KR_{vir}-G_cG_iG_{LR}G_{mgload}G_{output}KR_{vir}$$
$$-G_cG_iG_{LR}G_{mgload}G_vKR_{vir}-G_cG_iG_{line}G_{LR}G_{output}G_vKR_{vir}$$

$$\beta=1+G_cG_{LR}+GcG_{output}+G_iG_{LR}K+G_cG_iG_{LR}G_{output}K+G_cG_iG_{LR}G_vK+G_{line}R_{vir}+GcGlineG_{LR}R_{vir}+G_{mgload}R_{vir}+GcG_{LR}G_{mgload}R_{vir}$$
$$+G_{output}R_{vir}+G_cG_{line}G_{output}R_{vir}+G_cG_{LR}G_{output}R_{vir}+G_cG_{mgload}G_{output}R_{vir}+G_iG_{line}G_{LR}KR_{vir}+G_iG_{LR}G_{mgload}KR_{vir}+G_iG_{LR}G_{output}KR_{vir}$$
$$+G_cG_iG_{line}G_{LR}G_{output}KR_{vir}+G_cG_iG_{LR}G_{mgload}G_{output}KR_{vir}+G_cG_iG_{line}G_{LR}G_vKR_{vir}+G_cG_iG_{LR}G_{mgload}G_vKR_{vir}+G_cG_iG_{LR}G_{output}G_vKR_{vir}$$
$$+G_cG_iG_{LR}G_{output}G_{\sec}G_vKR_{vir}$$

REFERENCES

[1] LI Yunwei, Nejabatkhah F, "Overview of control, integration and energy management of microgrids, Journal of Modern Power Systems and Clean Energy, vol. 2, no. 3, pp. 212-222. 2014.

[2] Hatziargyriou, N., Asano, H., Iravani, R., Marnay, C.Microgrids, "MicroGrids," Power and Energy Magazine, IEEE on, vol. 5, no. 4, pp. 78-94, Jul. 2007

[3] Bidram, A., Davoudi, A., "Hierarchical Structure of Microgrids Control System," Smart Grid, IEEE Transactions on, vol. 3, no.4, pp. 1963-1976, Dec. 2012.

[4] Xiaonan Lu, Guerrero, J.M., Kai Sun, Vasquez, J.C., "Hierarchical Control of Parallel AC-DC Converter Interfaces for Hybrid Microgrids," Smart Grid, IEEE Transactions on, vol. 5, no. 2, pp. 683-692, Dec. 2014.

[5] Shafiee, Q., Guerrero, J.M., Vasquez, J.C. "Distributed Secondary Control for Islanded Microgrids—A Novel Approach," Power Electronics, IEEE Transactions on, vol. 29, no. 2, pp. 1018-1031, Apr. 2013.

[6] Shichao Liu, Xiaoyu Wang, Liu, P.X, "Impact of Communication Delays on Secondary Frequency Control in an Islanded Microgrid," Industrial Electronics, IEEE Transactions on, vol. 62, no. 4, pp. 2021 - 2031, Nov. 2014.

[7] Bidram, A., Davoudi, A., Lewis, F.L., "Distributed Cooperative Secondary Control of Microgrids Using Feedback Linearization," Power Systems, IEEE Transactions on, vol. 28, no. 3, pp. 3462-3470, Mar. 2013.

[8] Fanghong Guo, hangyun Wen, ianfeng Mao," Distributed Secondary Voltage and Frequency Restoration Control of Droop-Controlled Inverter-Based Microgrids," Industrial Electronics, IEEE Transactions on, vol. 62, no. 7, pp. 4355-4364, Dec. 2014.

[9] Tzung-Lin Lee, Po-Tai Cheng, "Design of a New Cooperative Harmonic Filtering Strategy for Distributed Generation Interface Converters in an Islanding Network," Power Electronics, IEEE Transactions on, vol. 22, no. 5, pp. 1919-1927, Sep. 2007.

[10] Hamzeh, M., Karimi, H., Mokhtari, H., "Harmonic and Negative-Sequence Current Control in an Islanded Multi-Bus MV Microgrid," Smart Grid, IEEE Transactions on, vol. 5, no. 1, pp. 167-176, Jun. 2014.

[11] Jinwei He, Yun Wei Li, Blaabjerg, F. "An Enhanced Islanding Microgrid Reactive Power, Imbalance Power, and Harmonic Power Sharing Scheme," IEEE Transactions on Power Electronics, vol. 30, no. 6, pp. 3389-3401, Jun. 2014.

[12] Savaghebi, M., Jalilian, A., Vasquez, J.C, "Secondary Control Scheme for Voltage Unbalance Compensation in an Islanded Droop-Controlled Microgrid," Smart Grid, IEEE Transactions on, vol. 3, no. 2, pp. 797-807, Feb. 2012.

[13] Savaghebi, M., Jalilian, A., Vasquez, J.C., "Secondary Control for Voltage Quality Enhancement in Microgrids," Smart Grid, IEEE Transactions on, vol. 3, no. 4, pp. 1893-1902, Jul. 2012.

[14] Quanwei Liu; Yong Tao; Xunhao Liu; Yan Deng; Xiangning He, "Voltage unbalance and harmonics compensation for islanded microgrid inverters," Power Electronics, IET, vol. 7, no. 5, pp. 1055-1063, May. 2014.

[15] Josep M. Guerrero, José Matas, Luis García de Vicuña, Miguel Castilla, Jaume Miret, "Wireless-Control Strategy for Parallel Operation of Distributed-Generation Inverters," Industrial Electronics, IEEE Transactions on, vol.53, no.5, pp.1461-1470, Oct. 2006.

[16] Mohammad S. Golsorkhi, Dylan D. C. Lu, "A Control Method for Inverter-Based Islanded Microgrids Based on V-I Droop Characteristics,"

Power Delivery IEEE Transactions on, vol.30, no.3, pp.1196,-1204, June. 2015.
[17] Guerrero, J.M.; Chandorkar, M.; Lee, T.; Loh, P.C., "Advanced Control Architectures for Intelligent Microgrids—Part I: Decentralized and Hierarchical Control," Industrial Electronics, IEEE Transactions on, vol. 60, no. 4, pp. 1254-1262, Apr. 2013
[18] Jinwei He, Yun Wei Li, Munir, M.S, "A Flexible Harmonic Control Approach through Voltage-Controlled DG–Grid Interfacing Converters," Industrial Electronics, IEEE Transactions on, vol. 59, no. 1, pp. 444-455, Apr. 2011.
[19] Jinwei He, Yun Wei Li, Blaabjerg, F., "Flexible Microgrid Power Quality Enhancement Using Adaptive Hybrid Voltage and Current Controller," Industrial Electronics, IEEE Transactions on, vol. 61, no. 6, pp. 2784-2794, Sep. 2013.
[20] Jinwei He, Beihua Liang, "Direct Microgrid Harmonic Current Compensation and Seamless Operation Mode Transfer Using Coordinated Triple-Loop Current-Voltage-Current Controller," IEEE 8th International Power Electronics and Motion Control Conference, 2016 , IPEMC-ECCE Asia, May 2016.
[21] Alexander Micallef, Maurice Apap, Cyril Spiteri-Staines, etc, "Reactive Power Sharing and Voltage Harmonic Distortion Compensation of Droop Controlled Single Phase Islanded Microgrids, "IEEE Transactions on Smart Grid, vol. 5, no. 3, pp. 1149 - 1158. 2014.
[22] Xiongfei Wang; Frede Blaabjerg, "Autonomous Control of Inverter-Interfaced Distributed Generation Units for Harmonic Current Filtering and Resonance Damping in an Islanded Microgrid," IEEE Transactions on Industry Applications, vol. 50, no. 1, pp. 452 - 461. 2014.

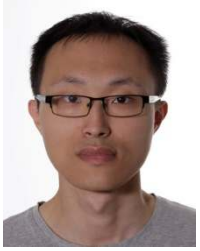

Wei Feng (S'16) received the B.Sc. and M.Sc. degrees in Automation from the Beijing Jiaotong University, Beijing, China, in 2006 and 2008, respectively. He received the Ph.D. degree in power electronics and motor drive from the Institute of Electrical Engineering, Chinese Academy of Sciences, Beijing, in 2014. He is currently a Post-Doc in Tsinghua University, China. His research interests include control of paralleled inverters for renewable generation systems, power quality improvement and energy management system for microgrids.

Kai Sun (M'12-SM'16) received the B.E., M.E., and Ph.D. degrees in electrical engineering from Tsinghua University, Beijing, China, in 2000, 2002, and 2006, respectively.

He joined the faculty of Electrical Engineering, Tsinghua University, in 2006, where he is currently an AssociateProfessor. From 2009 to 2010, he was a Visiting Scholar of Electrical Engineering with the Department of Energy Technology, Aalborg University, Aalborg, Denmark. His current research interests include power electronics for renewable generation systems, microgrids, and active distribution networks.

Dr. Sun is a member of IEEE Power Electronics Society Sustainable Energy Systems Technical Committee, a member of IEEE Power Electronics Society Power and Control Technology Committee, and a member of IEEE Industrial Electronics Society Renewable Energy Systems Technical Committee. He is an Associate Editor for the JOURNAL OF POWER ELECTRONICS. He was a recipient of the Delta Young Scholar Award in 2013.

Yajuan Guan (S'14) received the B.S. degree and M.S. degree in Electrical Engineering from the Yanshan University, Qinhuangdao, Hebei, China, in 2007 and 2010 respectively, and received Ph.D. degree in Electrical Engineering from the Aalborg University, Aalborg, Denmark, in 2016. From 2010 to 2012, she was an Assistant Professor in Institute of Electrical Engineering (IEE), Chinese Academy of Sciences (CAS). Since 2013, she has been a Lecturer in IEE; CAS. She is currently a Post-Doc at the Department of Energy Technology, Aalborg University, Denmark, as part of the Denmark Microgrids Research Programme (www.microgrids.et.aau.dk).

Her research interests include microgrids, distributed generation systems, power converter for renewable energy generation systems, and ancillary services for microgrids.

Josep M. Guerrero (S'01–M'04–SM'08–F'15) received the B.S. degree in telecommunications engineering, the M.S. degree in electronics engineering, and the Ph.D. degree in power electronics from the Technical University of Catalonia, Barcelona, Spain, in 1997, 2000, and 2003, respectively. Since 2011, he has been a Full Professor at the Department of Energy Technology, Aalborg University, Aalborg, Denmark, where he is responsible for the Microgrid Research Program; since 2012, he has been a Guest Professor at the Chinese Academy of Science, Beijing, China, and the Nanjing University of Aeronautics and Astronautics, Nanjing, China; since 2014, he has been a Chair Professor at Shandong University, Jinan, China; and since 2015, he has been a Distinguished Guest Professor at Hunan University, Changsha, China. His research interests include different microgrid aspects, including power electronics, distributed energystorage systems, hierarchical and cooperative control, energy management systems, and optimization of microgrids and islanded minigrids. Prof. Guerrero is an Associate Editor of the IEEE TRANSACTIONS ON POWER ELECTRONICS, the IEEE TRANSACTIONS ON INDUSTRIAL ELECTRONICS, and the IEEE INDUSTRIAL ELECTRONICS MAGAZINE, and an Editor of the IEEE TRANSACTIONS ON SMART GRID and the IEEE TRANSACTIONS ON ENERGY CONVERSION. He has been a Guest Editor of the IEEE TRANSACTIONS ON POWER ELECTRONICS Special Issues: the Power Electronics for Wind Energy Conversion and the Power Electronics for Microgrids; the IEEE TRANSACTIONS ON INDUSTRIAL ELECTRONICS Special Sections: the Uninterruptible Power Supplies systems, the Renewable Energy Systems, the Distributed Generation and Microgrids, and the Industrial Applications and Implementation Issues of the Kalman Filter; and the IEEE TRANSACTIONS ON SMART GRID Special Issue on the Smart DC Distribution Systems. He was the Chair of the Renewable Energy Systems Technical Committee of the IEEE Industrial Electronics Society. In 2014, he received the award of Highly Cited Researcher by Thomson Reuters.

Xi Xiao (M'07) was born in Hunan Province, China, in 1973. He received the B.E., M.E., and Ph.D. degrees in electrical engineering from Saint Petersburg State Technical University, Saint Petersburg, Russia, in 1995, 1997, and 2000, respectively.

Since 2001, he has been with the Department of Electrical Engineering and Applied Electronic Technology, Tsinghua University, Beijing, China, where he is currently a Full Professor and the Vice Dean of the Department. His main areas of research interest are motor control, power electronics and renewable energy.